

# A review on the main approaches for determination of the multiaxial high cycle fatigue strength

José C. Balthazar and Lucival Malcher

*Department of Mechanical Engineering, University of Brasilia, DF – Brazil*

## Abstract

The estimation of fatigue strength or fatigue life of a component under combined loading is fundamental to correct design and safe operational life of many structural components. The fatigue process under complex states of stresses generated in these situations is known as Multiaxial Fatigue. In the present work the different theories proposed to predict fatigue strength under in-phase and out-of-phase combined loading are reviewed. Special attention is given to new approaches for out-of-phase loading based on the stress invariant method.

Keywords: fatigue strength, multiaxial loading, out-of-phase loading, stress invariant method

## 1 Introduction

Most of structural mechanical components are frequently subjected to variable loading, which can lead to sudden fatigue failure. Crank drive shafts, pressure vessels, blade/rotor junctions, bolted junctions and many aeronautical components are usually operating under combined loads which can still be out of phase and in different frequencies generating complex biaxial or triaxial states of stresses. The fatigue process under such states of stresses is known as Multiaxial Fatigue whose consideration is of fundamental importance for assessment of life and operational reliability of structural components. Therefore, efficient and accurate methodologies for the evaluation of fatigue endurance limit under multiaxial stress states are required for use in engineering design applications.

Although many important developments have been made over more than hundred years of research on the subject, many designers still resort to large factors of safety to guard structural components against fatigue failures. The first attempts to investigate problems of multiaxial fatigue go back to the end of 19<sup>th</sup> century when Lanza [1] published results of tests concerning combined bending/torsion loading. In the early decades of the 20<sup>th</sup> century, investigators like Mason [2], Haigh [3], Nishiara and Kawamoto [4] and Gough *et al* [5] presented empirical relations obtained from experimental data. The initial theories proposed to predict fatigue failure under combined loading were basically an extension of the failure theories for static multiaxial state of stress to multiaxial states of cyclic stresses. The aim of these theories was to produce an uniaxial stress amplitude equivalent to a given multiaxial

cyclic stress state and then use it to predict fatigue life from S-N curves, obtained from conventional fatigue tests. The Maximum Shearing Stress Theory of Fatigue Failure and the Distortion Energy Multiaxial Theory of Fatigue Failure [6] were basically extensions of the Tresca and von Mises theories, respectively. The stress amplitudes were substitutes for the static principal stresses and the reversed fatigue strength or fatigue limit replaced the yield stress. The experimental evidence showed these methods were very conservative. The models for multiaxial fatigue analysis are generally divided into three groups: the stress-based models, strain-based models and energy models.

For multiaxial high cycle fatigue – HCF analysis, a number of criteria, derived from different approaches to the problem, have been reviewed in the literature [7,8], the equivalent stress, the critical plane, the average stress and the stress invariant methods, are the most known approaches for the problem.

In the present work, some of the proposed criteria to assess the fatigue resistance of structural components under multiaxial stress states in the HCF regime are presented underlying the fundamental principles on which they are based.

## 2 Multiaxial high cycle fatigue models

Many mechanical components, like the hydraulic turbines used in the power generating industry, are designed to endure a very large number of cycles without failure. Their size and operational conditions make impractical frequent stoppages for inspection and maintenance and, consequently, the use of Fracture Mechanics approaches for failure control. In the high cycle fatigue regime, most of total life is spent to initiate a crack of detectable size by non-destructive inspection. Thus, in these cases, it would be preferable to design against HCF, considering a criterion for crack initiation in order to keep structures under dynamic loading operating safely. To achieve this objective, a domain of safety, limited by a threshold below which cracks will not initiate, must be calculated.

The degradation of the state of the material under HCF occurs at stress levels well below the yield limit. The fatigue damage is related to cyclic plastic deformations at the grain level, followed by the formation of persistent slip bands from which microcracks will be nucleated, even in materials under elastic regime at macroscopic level. Therefore, shear stresses must be considered as one of the driving forces of the fatigue process. The normal stresses, which act upon the initiating crack, will also affect the fatigue resistance.

### 2.1 The equivalent stress theories

The equivalent stress or strain methods consists basically of determining an uniaxial stress or strain amplitude which would produce the same fatigue life as the multiaxial cyclic stress states, then this equivalent stress is used to predict fatigue life from conventional S-N curves.

The models of Sines [9] and Crossland [10] are examples of this kind of theory. The criterion of Sines [9] is expressed in terms of octahedral-shear stress as a linear function of the sum of the orthogonal

normal static stresses:

$$\frac{1}{3} \{(\sigma_{1a} - \sigma_{2a})^2 + (\sigma_{2a} - \sigma_{3a})^2 + (\sigma_{1a} - \sigma_{3a})^2\}^{\frac{1}{2}} \leq A - \alpha(\sigma_{xm} + \sigma_{ym} + \sigma_{zm}) \quad (1)$$

where  $\sigma_{1a}$ ,  $\sigma_{2a}$  and  $\sigma_{3a}$  are the alternating principal stress on the directions 1,2 and 3;  $\sigma_{xm}$ ,  $\sigma_{ym}$  and  $\sigma_{zm}$  are the normal mean stress on the directions  $x$ ,  $y$  and  $z$ ;  $A$  and  $\alpha$  are material constants, being  $A$  proportional to the reversed fatigue strength and  $\alpha$  gives the variation of the permissible range of stress with static stress. For a biaxial state of stress, Equation (1) delimits an ellipse whose size depends on the sum of the static (mean) stresses ( $\sigma_{xm} + \sigma_{ym}$ ). The region inside the ellipse is the safe region and any combination of loads which produce alternate stresses within this area will not have premature failure.

The Crossland criterion [10] differs from Sines criterion by considering the maximum value of the hydrostatic stress instead of its mean value. These criteria predict whether a fatigue crack may develop under given fatigue loading conditions, but they fail in considering the material physical stress-strain response in terms of crack nucleation and growth. Their applicability is limited to cases in which the principal axes of the alternating components are fixed to the body. Both criteria can also be expressed in terms of stress invariants, as will be shown below. Similar methods were proposed using the equivalent alternating strain as independent variable, instead of stress, and then used for low cycle fatigue by entering an  $\varepsilon-N$  curve.

## 2.2 The critical planes theories

Fatigue cracks initiate in planes of maximum shear and propagate through the grains whose irregular surfaces would difficult the crack growth due to mechanical interlocking and friction effects. But normal stresses and strains acting upon the crack planes would open the crack, allowing it to grow. From this point of view the stresses and strains on the most severely loaded planes in the material would govern the fatigue process as cracks nucleates in a plane where the amplitude or the value of some stress components or a combination of them reach its maximum value with the tensile and compressive mean stresses having, respectively a detrimental or beneficial effect on fatigue life. These observations led to the proposal of several theories known as the critical plane methods. Along the load cycle, the stresses and strains are determined on several planes and applying some criterion, the more severely loaded plane, or critical pane, where the fatigue cracks are expected to nucleate, is then identified. This criterion will also give a measure of the fatigue damage, which will be used to predict fatigue life. Findley [11], among the first to use the critical plane concept, postulated that normal stresses acting on planes of maximum shear would affect the fatigue damage process. Brown and Miller [12] suggested that the parameters governing the fatigue process were the maximum shear and normal strain acting on those planes. However, Socie[13] showed that for non-proportional loading, the cyclic hardening of the material would affect the fatigue process leading to smaller fatigue lives. Besides, Socie [13] and Fatemi and Socie [14] showed the cracks could grow on these planes in different ways, mode I or mode II, depending on the type of loading, magnitude of strain and the materials characteristics. Brown and Miller [12] stated also on mode II the cracks could grow on these planes in two different ways: type A cracks would propagate along the surface and type B cracks would propagate away from the

surface. As the way the cracks will grow is not known in advance it would be necessary to consider both situations making calculations for the two possible modes of cracking. The shear strain of model of Socie [13], the normal strain model of Fatemi and Socie [14] and the shear stress model proposed by McDiarmid [15] are characteristic of this approach.

The model proposed by Socie [13] is basically an extension of the fatigue parameter proposed by Smith, Watson and Topper [16], for the case of cracks that grow in planes of high tensile stress (mode I), expressed as:

$$\sigma_{\max}\varepsilon_{1a} = \sigma'_f\varepsilon'_f(2N_f)^{c+b} + \left(\frac{\sigma'_f}{E}\right)(2N_f)^{2b} \quad (2)$$

where  $\varepsilon_{1a}$  is the amplitude of the principal strain and  $\sigma_{max}$  is the maximum (mean + alternate) stress acting on the plane of  $\varepsilon_{1a}$ . The right side of equation (2) is the description of a  $\varepsilon-N$  curve and the left side represents the loading variables for the plane of the greatest amplitude of normal strain (principal strain). For situations where the cracks grow on planes of high shear stress (mode II) Fatemi and Socie [14] suggested the following relationship:

$$\gamma_{ac} \left(1 + \frac{\alpha\sigma_{\max}}{\sigma'_y}\right) = \frac{\tau'_f}{G}(2N_f)^b + \gamma'_f(2N_f)^c \quad (3)$$

where  $\gamma_{ac}$  is the largest amplitude of shear strain for any plane;  $\sigma_{max}$  is the peak tensile stress normal to the plane of  $\gamma_{ac}$ , occurring any time during the  $\gamma_{ac}$  cycle;  $\alpha$  is an empirical constant and;  $\sigma'_y$  is the cyclic yield strength. The terms of the left side of equation (3) represent the loading variables and  $\tau'_f$ ,  $b$ ,  $\gamma'_f$  and  $c$  defines the strain-life curve from completely reversed tests in pure shear.

Different from Brown and Miller [12] and Socie [13], McDiarmid [15] assume the plane maximum shear stress amplitude as the critical plane and the maximum shear stress amplitude on that plane the main responsible for fatigue crack growth. His model also take into account the effect of the maximum normal stress on that plane on the crack growth process. The model of McDiarmid [15] is expressed as:

$$\frac{\tau_{a,\max}}{t_{-1}} + \frac{\sigma_{a,\max}}{2.S_{ut}} = 1 \quad (4)$$

where  $\tau_{a,\max}$  and  $\sigma_{a,\max}$ , are the maximum amplitude of shear and normal stress, respectively, on the plane of maximum shear stress amplitude,  $t_{-1}$  is the fatigue limit under reversed torsion and  $S_{ut}$  is the ultimate tensile strength. Other theories based on the critical plane approach have been reviewed by Kussmaul, McDiarmid and Socie [17] and Karolczuk and Macha [18].

These methods present some difficulties to implement, as most of them require a number of parameters to be determined experimentally from different types of fatigue tests. If plastic deformations are involved, as in low cycle fatigue, the characterization of the plastic behaviour of the materials have to be done through a plasticity theory which adds an extra complexity to the method implementation. The different modes of crack growth require the consideration of different possibilities in the analysis. As the way the cracks will grow is not known in advance it would be necessary to consider both situations, mode I or mode II, making calculations for the possible modes of cracking. Some models do not distinguish the different types of crack growth, losing the relation with the physical interpretation,

which is the great appeal of this approach. The critical plane models based on strain do not give good results for high cycle fatigue as, in this situation, the fatigue process is controlled by elastic stresses.

### 2.3 The average stress theories

The average stress approach is based on the averages of normal and shear stresses acting on a generic material plane within an elementary volume. This quantity is treated as an equivalent stress and correlated to the fatigue damage. Papadopoulos et al [19] proposed a fatigue criterion based on the average values of the normal stress  $N$  and of the shear stress  $T_a$  within an elementary volume  $V$ :

$$\sqrt{\langle T_n^2 \rangle} + \alpha \left( \max_t \langle N \rangle \right) \leq \beta \quad (5)$$

where  $T_n$  is the root mean square of the shear stress amplitude within a volume  $V$ ,  $\max_t \langle N \rangle$  is the maximum value that the spatial mean normal stress reaches during the loading cycle, and  $\alpha, \beta$  are material constants to be derived from the fully reversed endurance limits,  $f_{-1}$  and  $t_{-1}$ , for bending and torsion, respectively. The formula is similar to Crossland's criterion except by the second invariant of the stress deviator, which is replaced by the average stress quantity. This model is limited to materials in which the relation  $t_{-1}/f_{-1}$  is between 0.577 and 0.8. Non-proportional loading has no effect on Eq. (5), which is in conflict with experimental observations made by You and Lee [20].

Papadopoulos [21] improved the model using a critical plane type model:

$$\max (T_a^\Delta) + \lambda [(J_1)_a + (J_1)_m] = \beta \quad (6)$$

where  $J_1$  is the first invariant of the stress tensor and the subscripts  $a$  and  $m$  refer to the stress amplitude and mean stress, respectively.  $T_a^\Delta$  is an average stress quantity, named generalized shear stress amplitude, on the critical plane  $\Delta$ . The critical plane is defined as the plane  $\Delta$  where  $T_a$  achieves the maximum value. Other average stress approaches were proposed by Grubisic and Simburger [22].

Dang Van *et al* [23] and Papadopoulos [24] proposed other criteria based on a local stress analysis approach, which assumes that localized plastic deformation in a critically oriented plane would lead to crack initiation. The local microscopic stresses, expressed as function of the macroscopic stresses, are used to define a crack initiation criterion.

Reviewing the subject, Papadopoulos [25] observed the average stress models yield good estimations for in-phase loading but they are imprecise for out-of-phase loading, where the principal stress and strain axis change direction along the time, condition which influences the fatigue phenomena.

### 2.4 The stress invariant methods

The invariant stress approach is based on the invariants of the stress tensor and/or its deviator tensor. The basic idea is to directly relate the fatigue strength with the second invariant of the stress deviator and first invariant of the stress (3 times the hydrostatic stress). The initiation of a fatigue crack under cyclic loading would be predicted when the left side of the equation below gets bigger than the right side:

$$\sqrt{J_{2,a}} + k(N) \cdot \sigma_H \leq \lambda(N) \quad (7)$$

where:  $\sqrt{J_{2,a}}$  is the equivalent shear stress amplitude,  $\sigma_H$  is the hydrostatic stress and  $k(N)$  and  $\lambda(N)$  are parameters to be experimentally determined.

Some models which use only the first invariant of the stress tensor and the second invariant the deviator tensor can be regarded as a combination of the equivalent stress approach, as it uses a shear stress equivalent to the multiaxial applied stresses, and the critical plane approach, as it searches for the maximum values of their parameters in a plan with the greatest intersection with the path of the deviator stress tensor. The models of Sines [9], Crossland [10] and Kakuno-Kawada [26] can be also be classified in this category are good representatives of this kind of approach.

The criteria of Sines [9] and Crossland [10] can be written in a general form as:

$$g(\tau) + f(\sigma) \leq \lambda \quad (8)$$

where,  $f$  and  $g$  are functions of the shear stress  $\tau$  and the normal stress  $\sigma$ , respectively. The Sines [9] criterion is mathematically expressed as:

$$\sqrt{J_{2,a}} + k\sigma_{H,mean} \leq \lambda \quad (9)$$

where  $\sqrt{J_{2,a}}$  is the equivalent shear stress amplitude and  $\sigma_{H,mean}$  is the mean hydrostatic stress. The parameters  $k$  and  $\lambda$  are material constants, which can be obtained from two simple fatigue tests: the repeated bending limit  $f_0$  ( $\sigma_a = \sigma_m = f_0$ ) and the fully reversed torsion limit  $t_{-1}$  ( $\tau_a = t_{-1}$ ,  $\tau_m = 0$ ).

$$k = \left( \frac{3t_{-1}}{f_0} \right) - \sqrt{3} ; \quad \lambda = t_{-1} \quad (10)$$

Instead of the mean hydrostatic stress, the Crossland [9] criterion considers the influence of the maximum hydrostatic stress,  $\sigma_{H,max}$ :

$$\sqrt{J_{2,a}} + k\sigma_{H,max} \leq \lambda \quad (11)$$

The parameters  $k$  and  $\lambda$  can be also obtained from two simple fatigue tests: the fully reversed bending limit  $f_{-1}$  ( $\sigma_a = f_{-1}$ ,  $\sigma_m = 0$ ) and the fully reversed torsion limit  $t_{-1}$  ( $\tau_a = t_{-1}$ ,  $\tau_m = 0$ ).

$$k = \left( \frac{3t_{-1}}{f_{-1}} \right) - \sqrt{3} ; \quad \lambda = t_{-1} \quad (12)$$

Kakuno and Kawada [26] suggested that the contribution of the invariant of the stress deviator and the hydrostatic stress should be different:

$$\sqrt{J_{2,a}} + k.\sigma_{H,a} + \lambda.\sigma_{H,m} \leq \mu \quad (13)$$

where the parameters  $k$ ,  $\lambda$  and  $\mu$  should be determined from three uniaxial fatigue limits:  $f_0$ ,  $t_{-1}$  e  $f_{-1}$  (repeated bending, fully reversed torsion, fully reversed bending). Thus,

$$k = \left( \frac{3t_{-1}}{f_{-1}} \right) - \sqrt{3} \quad (14)$$

$$\lambda = \left( \frac{3t_{-1}}{f_0} \right) - \sqrt{3} \quad (15)$$

$$\mu = t_{-1} \quad (16)$$

For these criteria, failure will occur when the left side of the equation gets greater than the right side.

### 3 The equivalent shear stress amplitude

The basic difference in the application of the models based on the invariants of the stress tensors, as the models of Sines [9], Crossland [10] and Kakuno-Kawada [26], is the value, mean or maximum, of the hydrostatic stress  $\sigma_H$  used and the way to calculate the parameter  $\sqrt{J_{2,a}}$ . The definition of hydrostatic stress is well established and no greater difficulty to calculate it exists. The definition of the equivalent shear stress amplitude  $\sqrt{J_{2,a}}$  is more complicated.

When the applied cyclic loading is uniaxial or in-phase multiaxial, the equivalent shear stress amplitude  $\sqrt{J_{2,a}}$  can be determined directly taking the square root of the second invariant of the deviatory tensor:

$$\sqrt{J_{2,a}} = \sqrt{\frac{1}{6} \left\{ (\sigma_{xx,a} - \sigma_{yy,a})^2 + (\sigma_{yy,a} - \sigma_{zz,a})^2 + (\sigma_{zz,a} - \sigma_{xx,a})^2 + 6 \cdot (\tau_{xy,a}^2 + \tau_{yz,a}^2 + \tau_{xz,a}^2) \right\}} \quad (17)$$

However, when the applied cyclic loading is out-of-phase multiaxial, the determination of  $\sqrt{J_{2,a}}$  is not so simple, requiring complex mathematical calculations. The vector representing the equivalent shear stress amplitude has its direction and magnitude varying along the cycle. Fig. 1 shows how the shear stress amplitude varies along the cycle on a proportional and non-proportional loading;

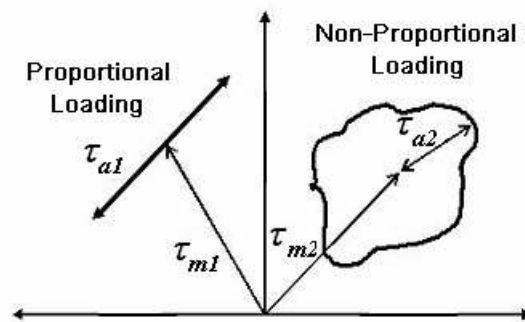


Figure 1: Behaviour of the shear stress amplitude under proportional and non-proportional loading.

On the point under study, a generic plane  $\Delta$  can be defined by its unit normal vector  $\mathbf{n}$ , described by the spherical angles  $\phi$  and  $\theta$ , Fig. 2. The stress vector  $\mathbf{S}_n$  acting on a such plane can be decomposed in its normal vector  $\mathbf{N}$  and the shear stress vector  $\mathbf{C}$ .

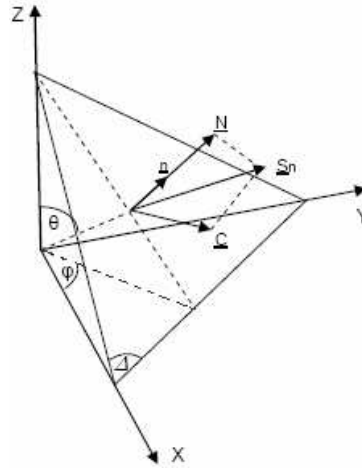


Figure 2: Stress vector  $\mathbf{S}_n$ , normal stress  $\mathbf{N}$  and shear stress vector  $\mathbf{C}$  acting on generic plane  $\Delta$ . Bin Li *et al* [27].

During the load cycle, the tip of the vector  $\mathbf{S}_n$  describes a closed space curve  $\psi$  whose projection on plane  $\Delta$  is the path of the shear stress vector  $\mathbf{C}$  on that plane,  $\psi'$ , Figure 3. The shear stress amplitude  $C_a$  depends on the orientation of plane  $\Delta$ , thus  $C_a = f(\phi, \theta)$ . To determine the maximum shear stress amplitude  $C_{a,max}$  is necessary to search the maximum of  $C_a = f(\phi, \theta)$  over the angles  $\phi$  and  $\theta$ . The critical plane approach requires to find the normal stress and shear stress amplitudes and mean values on each plane  $\Delta$  passing by the point of interest and then searching the critical plane. For stress invariant approaches, the amplitude of the equivalent shear stress  $\sqrt{J_{2,a}}$  remains the same for any orientation of the plane  $\Delta$ .

Different methods to calculate the equivalent shear stress amplitude were proposed by Dang Van *et al* [28], Deperrois [29], Duprat *et al* [30], Bin Li *et al* [27], Mamiya and Araújo [31] and Balthazar and Malcher [32] which will be described next.

### 3.1 The minimum circumscribed hypersphere method

Dang Van and Papadopoulos [33] proposed the shear stress amplitude to be the radius  $C_a$  of the minimum hypersphere circumscribing the loading path  $\psi'$ . The mean value of the shear stress is the length of the vector  $\mathbf{w}$  that points from the origin  $O$  to the center of the minimum circumscribed hypersphere,  $C_m$ , Figure 4. To facilitate the calculation of  $\sqrt{J_{2,a}}$ , the following transformation is used

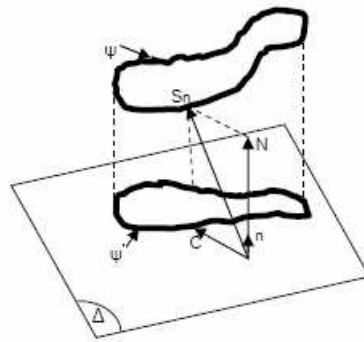


Figure 3: Load paths  $\psi$  described by the stress vector  $S_n$  and  $\psi'$  described by the shear stress vector  $C$  on a generic plane  $\Delta$ . Bin Li *et al* [27].

[34]:

$$S_1 = \frac{\sqrt{3}}{2} \bar{S}, \quad S_2 = \frac{1}{2} \left( \bar{S}_{yy} - \bar{S}_{zz} \right), \quad S_3 = \bar{S}_{xy}, \quad S_4 = \bar{S}_{xz}, \quad S_5 = \bar{S}_{yz} \quad (18)$$

With the above rules the general six components of the deviatoric stress may be transformed into a five component stress vector, allowing the stress deviator to be fully described by fewer components in the transformed space.

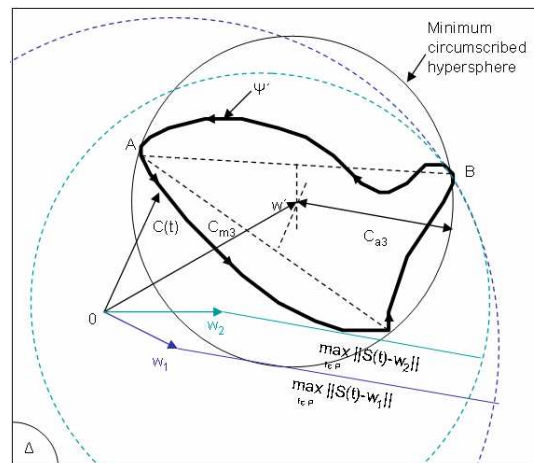


Figure 4: The Minimum Circumscribed Hypersphere. Dang Van and Papadopoulos [33].

The center  $w'$  and the radius  $R$  are determined by the following equations:

$$w' : \min_w (\max_t \|S(t) - w\|) \quad (19)$$

$$R = \max_t \|S(t) - w'\| \quad (20)$$

This method can produce inconsistent results, as for the load paths showed in Figure 5. The first load path is a non-proportional loading and the second is an in-phase proportional loading.

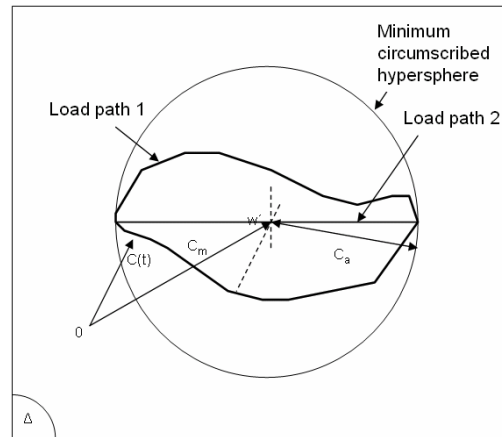


Figure 5: Example of a non-proportional loading and an in-phase proportional loading giving the same equivalent shear stress amplitude by the minimum circumscribed hypersphere method.

The two loadings will produce the same equivalent shear stress amplitude but they certainly would produce different fatigue damage. Other disadvantage is given by the need of complex computational implementation to calculate  $w'$  and  $C_a$ .

### 3.2 The minimum circumscribed ellipsoid method

An approach to determine the equivalent shear stress amplitude taking in account the effect of the phase angle was proposed by Bin Li *et al* [27]. Instead of circumscribing the loading path  $\psi'$  by a minimum hypersphere, Bin Li and his colleagues suggest to consider the minimum circumscribed ellipsoid to calculate  $\sqrt{J_{2a}}$ . The value of the equivalent shear stress would be then:

$$\sqrt{J_{2a}} = \sqrt{R_a^2 + R_b^2} \quad (21)$$

where  $R_a$  and  $R_b$  are the two semi-axis of an ellipse circumscribing the loading path  $\psi'$ . This method requires a two step procedure for the determination of  $\sqrt{J_{2a}}$ , figure 6. Firstly, a minimum circumscribed circle of radius  $R_a$ , equal to the ellipse great semi-axis, is established according the minimum

circumscribed hypersphere method, described above. The small semi-axis  $R_b$  is the determined from the minimum ellipse contained in the circle and also containing the loading path  $\psi'$ .

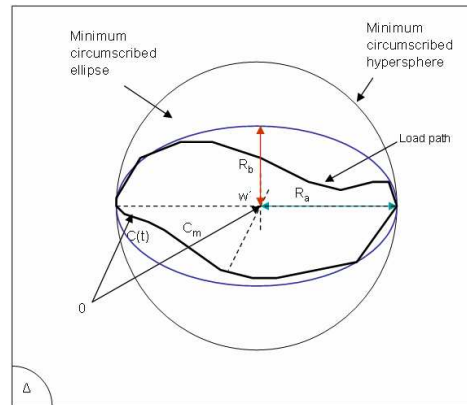


Figure 6: The minimum circumscribed ellipsoid method, Bin Li at al [27].

This model takes in account the effect of non-proportional loads on fatigue life and presents good results for multiaxial fatigue strength, when compared to the other methods, but it also presents the same difficulties of the Dang Van and Papadopoulos method to determine the center of the minimum circumscribed circle, which is also the center of the minimum circumscribed ellipse.

### 3.3 The minimum prismatic envelope method

Mamiya e Araújo [31] proposed, instead of hypersphere or a ellipsoid, the construction of an prismatic envelope containing the loading path projected on the deviatory plane, Figure 7. The equivalent shear stress amplitude could then be calculated by the following equation:

$$\sqrt{J_{2a}} = \left( \sum_{i=1}^5 a_i^2 \right)^{\frac{1}{2}} \quad (22)$$

where  $a_i$  are the amplitudes of the components  $x_i(t)$  of the microscopic deviatory stresses, defined as:

$$a_i = \max_i |x_i(t)| \quad (23)$$

### 3.4 The minimum simplified circumscribed ellipsoid method

Duprat *et al* [30] proposed a method, which could consider the phase angle in tension-bending and torsion stress loading. The model is derived from Crossland criteria, using the projection of the stress

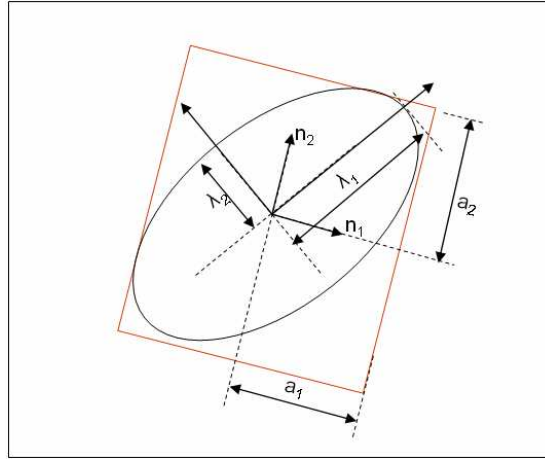


Figure 7: Ellipsoid in the  $R^m$  space and circumscribed rectangular prism arbitrarily oriented. Mamiya e Araújo [31].

tensor path on the deviatory plane. This projection is an ellipse of long axis  $D$  and short axis  $d$ , Figure 8. While Crossland original formula uses only  $D$  in the calculation of  $\sqrt{J_{2a}}$ , Duprat *et al* [30] replaces  $D$  by the half-perimeter of the ellipse,  $\frac{P_e}{2}$ , to take in account the phase difference, characterized by  $D$  and  $d$ .

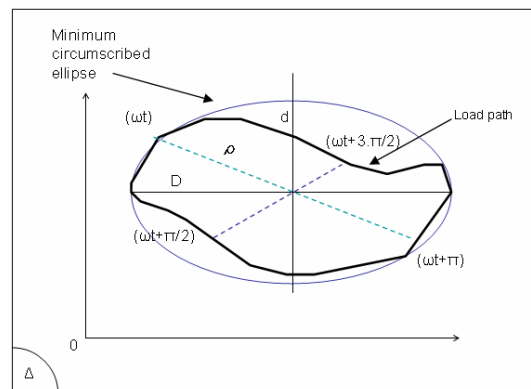


Figure 8: Projection of the tensor path on the deviatory plane. Duprat et al [30].

The values of  $D$  and  $d$  are given by:

$$D = \max(t) \rho(\omega t) \quad (24)$$

$$d = \min(t) \rho(\omega t) \quad (25)$$

with the parameter  $\rho(\omega t)$  being:

$$\rho(\omega t) = \text{tr} \left[ (\underline{S}(t) - \underline{S}(t + \pi)) \cdot (\underline{S}(t) - \underline{S}(t + \pi)) \right]^{\frac{1}{2}} \quad (26)$$

where  $\underline{S}(t)$  is the deviatoric stress tensor .

The value of the equivalent shear stress amplitude  $\sqrt{J_{2a}}$  is function of the ellipse half-perimeter  $p_e/2$ :

$$\sqrt{J_{2a}} = \frac{1}{2} \cdot \frac{p_e/2}{\sqrt{2}} \quad (27)$$

where

$$\frac{p_e}{2} \approx \frac{\pi}{2} \cdot \frac{D+d}{2} \cdot \left[ 1 + \frac{1}{4}\lambda^2 + \frac{1}{64}\lambda^4 + \frac{1}{256}\lambda^6 \right] \quad (28)$$

and

$$\lambda = \frac{D-d}{D+d} \quad (29)$$

Balthazar and Malcher [32] showed the application of this method results in increased scatter for larger phase angles between the applied loads. They showed that a reduction on such scattering could be obtained combining the proposal of Duprat *et al* [30] with the minimum circumscribed ellipsoid method proposed by Bin Li *et al* [27]. The equivalent shear stress amplitude could be calculated as proposed by Bin Li:

$$\sqrt{J_{2a}} = \sqrt{R_a^2 + R_b^2} \quad (30)$$

but using the values of the ellipse semi-axis from the model of Duprat. Thus:

$$R_a = \frac{D}{2} = \frac{\max(t) \rho(\omega t)}{2} \quad (31)$$

and

$$R_b = \frac{d}{2} = \frac{\min(t) \rho(\omega t)}{2} \quad (32)$$

The equivalent shear stress amplitude would be then given by:

$$\sqrt{J_{2a}} = \frac{1}{2} \frac{\sqrt{[\max(t) \rho(\omega t)]^2 + [\min(t) \rho(\omega t)]^2}}{\sqrt{2}} \quad (33)$$

The main advantage of this modification is the simplicity added to the equivalent shear stress amplitude calculations, as it is easier to determine the ellipse semi-axis  $D/2$  and  $d/2$  as proposed by Duprat than the complex calculations required to obtain the center of the minimum circumscribed

hypersphere or ellipsoid, necessary for the methods of Dang Van, Papadopoulos and Bin Li. Thus, the criterion for multiaxial fatigue can be expressed as:

$$\frac{1}{2} \frac{\sqrt{[\max(t) \rho(\omega t)]^2 + [\min(t) \rho(\omega t)]^2}}{\sqrt{2}} + \frac{\sqrt{3}}{S_{rt}} \cdot f_{-1} \cdot \sigma_{H,\max} \leq t_{-1} \quad (34)$$

#### 4 Critical analysis of the invariant stress methods

Experimental data obtained in the literature were used to assess the different criteria based on the invariant stress approach. It was used 32 results from constant amplitude combined bending + torsion loading, from in-phase and out-of-phase tests conducted by Nishihara and Kawamoto on hard steel (points 1 to 10); by Zenner *et al* on 34Cr4 steel (points 11 to 22) and by Froustey and Lasserre on 30NCD16 steel (points 23 to 32) as reported by Papadopoulos [19].

Defining the equivalent stress  $\sigma_{eq}$  to the fully reversed torsional fatigue limit  $t_{-1}$  ratio as  $K = \sigma_{eq}/t_{-1}$ , it is possible to assess the quality the predictions made by each model. If  $K=1$  the model predict perfectly the multiaxial fatigue behaviour. If  $K$  is higher than 1, the predictions are conservative. An index of error  $I$  can be also established as  $I = (K - 1) \times 100$ .

Tables 1 to 3 show the values of  $I$  and  $K$  for Crossland, Bin Li, Papadopoulos, Mamiya and Araújo, Duprat, and Balthazar and Malcher models. It can be observed that for the models of Bin Li, Papadopoulos, Mamiya and Araújo, and Balthazar and Malcher the maximum error lies around 6% while the Duprat model produces error up to 18% when the phase angle between the applied loads is  $90^\circ$ . The same pattern can be observed for the alloys 34Cr4 and 30NCD16 for all models except Crossland and Duprat models whose results present a larger scatter. It is clear that the model of Crossland does not contemplate the effect of the phase angle and the model of Duprat presents larger errors for larger phase angles. The models of Bin Li, Papadopoulos, Mamiya and Araújo, and Balthazar and Malcher present similar results with the difference lying on the method to calculate the equivalent shear stress amplitude  $\sqrt{J_{2a}}$ .

Papadopoulos tries to determinate this parameter through the minimum circle circumscribing the path of the deviatoric stress tensor,  $\psi'$ . For Bin Li  $\sqrt{J_{2a}}$  must be determined through the minimum ellipse circumscribing the path of the deviatoric stress tensor,  $\psi'$ . The main difficulty associated to these methods is the determination of the center of the circle or ellipse, which require complex calculations. The approach proposed by Mamiya and Araújo involves the use of a prismatic envelope of the load path to calculate  $\sqrt{J_{2a}}$ . It also requires complex calculations for the determination of the parameters  $a_i$ , which are equivalents of the amplitudes of the components  $x_i(t)$  of the microscopic deviatoric stresses. Notwithstanding the use of the idea of the circumscribed ellipsoid to calculate  $\sqrt{J_{2a}}$ , Balthazar and Malcher presents a simplified way to determine the equivalent shear stress amplitude, eliminating the need the complex calculations required by the other methods without losing quality in the results. Figure 7 shows the behaviour of the stress ratio  $K = \sigma_{eq}/t_{-1}$  for models analysed.

Table 1: Hard steel ( $t_{-1} = 196.2$  MPa,  $f_{-1} = 313.9$  MPa)

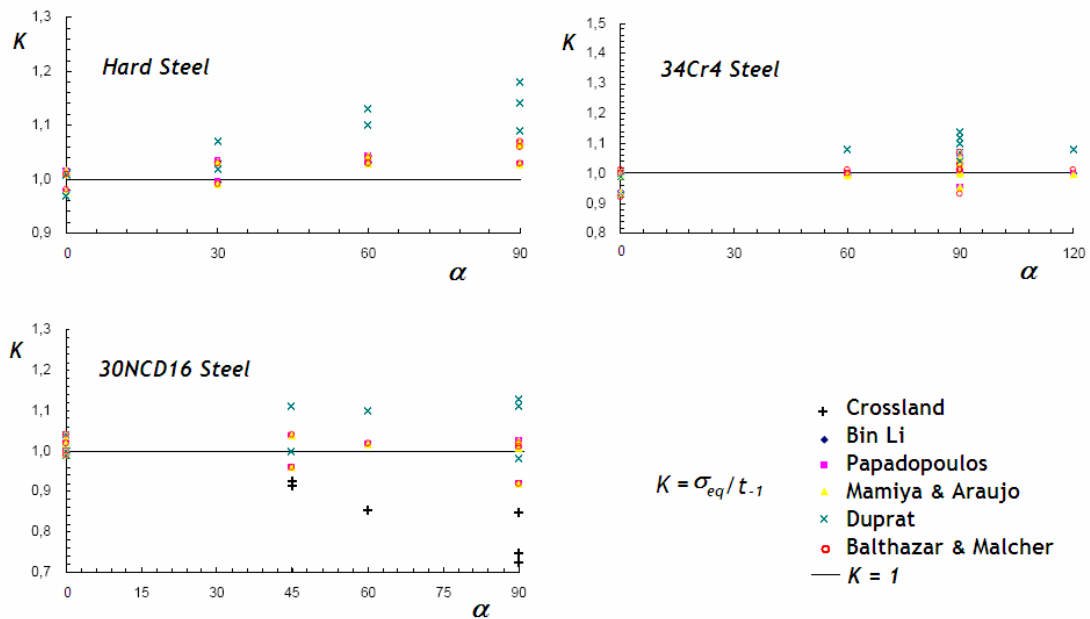
Test	$\sigma_{x,m}$	$\sigma_{x,a}$	$\tau_{xy,m}$	$\tau_{xy,a}$	$\alpha$	Bin Li		Papadopoulos		Mamiya & Araujo		Duprat		Balthazar & Malcher	
						K	I%	K	I%	K	I%	K	I%	K	I%
1	-	138.1	-	167.1	0	0.98	-2%	0.98	-2%	0.98	-2%	0.97	-3%	0.97	-2.7%
2	-	140.4	-	169.9	30	0.99	-1%	0.99	-1%	0.99	-1%	1.02	2%	0.99	-0.9%
3	-	145.7	-	176.3	60	1.03	3%	1.03	3%	1.03	3%	1.10	10%	1.03	3.4%
4	-	150.2	-	181.7	90	1.06	6%	1.06	6%	1.06	6%	1.14	14%	1.06	5.8%
5	-	245.3	-	122.6	0	1.02	1%	1.02	1%	1.01	1%	1.01	1%	1.01	1.3%
6	-	249.7	-	124.8	30	1.03	3%	1.03	3%	1.03	3%	1.07	7%	1.03	2.8%
7	-	252.4	-	126.2	60	1.04	4%	1.04	4%	1.04	4%	1.13	13%	1.04	4.1%
8	-	258.0	-	129.0	90	1.07	6%	1.07	6%	1.07	7%	1.18	18%	1.07	7.0%
9	-	299.2	-	62.8	0	1.01	1%	1.01	1%	1.01	1%	1.01	1%	1.01	1.3%
10	-	304.5	-	63.9	90	1.03	3%	1.03	3%	1.03	3%	1.09	9%	1.03	3.1%

Table 2: 34Cr4 steel ( $t_{-1} = 246$  MPa,  $f_{-1} = 410$  MPa)

Test	$\sigma_{x,m}$	$\sigma_{x,a}$	$\tau_{xy,m}$	$\tau_{xy,a}$	$\alpha$	Bin Li		Papadopoulos		Mamiya & Araujo		Duprat		Balthazar & Malcher	
						K	I%	K	I%	K	I%	K	I%	K	I%
11	-	314	-	157	0	0.99	-1%	0.99	-1%	0.99	-1%	0.99	-1%	0.99	-0.73%
12	-	315	-	158	60	1.00	0%	1.00	0%	1.00	0%	1.08	8%	0.99	-0.57%
13	-	316	-	158	90	1.00	0%	1.00	0%	1.00	0%	1.10	10%	1.00	-0.30%
14	-	315	-	158	120	1.00	0%	1.00	0%	1.00	0%	1.08	8%	0.99	-0.57%
15	-	224	-	224	90	1.05	5%	1.05	5%	1.05	5%	1.14	14%	1.05	4.68%
16	-	380	-	95	90	1.00	0%	1.00	0%	1.00	0%	1.07	7%	1.00	0.12%
17	-	316	158	158	0	1.00	0%	1.00	0%	1.00	0%	1.00	0%	1.00	0.27%
18	-	314	157	157	60	0.99	-1%	0.99	-1%	0.99	-1%	1.08	8%	0.99	-0.53%
19	-	315	158	158	90	1.00	0%	1.00	0%	1.00	0%	1.10	10%	1.00	-0.29%
20	279	279	-	140	0	0.94	-6%	0.94	-6%	0.94	-6%	0.93	-7%	0.93	-6.76%
21	284	284	-	142	90	0.95	-5%	0.95	-5%	0.95	-5%	1.04	4%	0.95	-5.26%
22	212	212	-	212	90	1.03	3%	1.03	3%	1.03	3%	1.12	12%	1.03	3.18%

Table 3: 30NCD16 steel ( $t_{-1} = 410$  MPa,  $f_{-1} = 660$  MPa)

Test	$\sigma_{x,m}$	$\sigma_{x,a}$	$\tau_{xy,m}$	$\tau_{xy,a}$	$\alpha$	Crossland		Papadopoulos		Mamiya & Araujo		Duprat		Balthazar & Malcher	
						K	I%	K	I%	K	I%	K	I%	K	I%
23	0	485	0	280	0	1.02	2%	1.02	2%	1.02	2%	1.01	1%	1.01	1.28%
24	0	485	0	277	90	0.73	-27%	1.01	1%	1.01	1%	1.11	11%	1.00	0.42%
25	300	480	0	277	0	1.04	4%	1.04	4%	1.04	4%	1.04	4%	1.04	4.28%
26	300	480	0	277	45	0.92	-8%	1.04	4%	1.04	4%	1.11	11%	1.04	4.24%
27	300	470	0	270	60	0.85	-15%	1.02	2%	1.02	1%	1.10	10%	1.01	1.39%
28	300	473	0	273	90	0.75	-25%	1.03	2%	1.02	2%	1.13	13%	1.03	2.57%
29	300	590	0	148	0	1.00	0%	1.00	0%	1.00	0%	1.00	0%	1.00	0.26%
30	300	565	0	141	45	0.91	-9%	0.96	-4%	0.96	-4%	1.00	0%	0.96	-3.97%
31	300	540	0	135	90	0.85	-15%	0.92	-8%	0.92	-8%	0.98	-2%	0.92	-8.10%
32	300	211	0	365	0	0.99	-1%	0.99	-1%	0.99	-1%	0.99	-1%	0.99	-0.73%

Figure 9: Stress ratio “K” versus phase angle  $\alpha$  for the models analysed. Malcher e Balthazar [32].

## 5 Conclusions

The different approaches to predict fatigue strength under in-phase and out-of-phase combined loading proposed by Dang Van et al [25], Deperrois [26], Duprat et al [28], Bin Li et al [29] and Mamiya e Araújo [30], were reviewed. Special attention was given to approaches for out-of-phase loading based on the stress invariant method and the different definitions and ways to calculate the equivalent shear stress amplitude  $\sqrt{J_{2a}}$ . A new simplified proposal to calculate this parameter, combining the proposal of Duprat *et al* [30] with the minimum circumscribed ellipsoid method of Bin Li *et al* [27], was presented. The new method to determine the equivalent shear stress amplitude eliminates the need the complex calculations required by the other methods without losing quality in the results.

## References

- [1] Lanza, G., Strength of shafting subjected to both twisting and bending. *Trans ASME*, **8**, pp. 121–196, 1886.
- [2] Mason, W., (ed.), *Alternating Stress Experiments*, IMechE, 1917.
- [3] Haigh, B.P., The thermodynamic theory of mechanical fatigue and hysteresis in metals. *Rep British Association for the Advancement of Science*, pp. 358–368, 1923.
- [4] Nishiara, T. & Kawamoto, M., *The Strength of Metals under Combined Alternating Bending and Torsion - Memoirs - College of Engineering*, volume 10. Kyoto Imp. University: Japan, 1941.
- [5] Gouch, H.J., Pollard, H. & Clenshaw, W.J., *Some Experiments on the Resistance of Metals to fatigue under Combined Stresses*. Aero Research Council - R&M 2522, 1951.
- [6] Collins, J.A., *Failure of Materials in Mechanical Design*. Wiley: New York - USA, 1981.
- [7] Garud, Y.S., Multiaxial fatigue: A survey of the state of the art. *J of Testing and Evaluation*, **9(3)**, pp. 165–178, 1981.
- [8] Wang, Y.Y. & Yao, W.X., Evaluation and comparison of several multiaxial fatigue criteria. *Int J Fatigue*, **26(1)**, pp. 17–25, 2004.
- [9] Sines, G., Failure of materials under combined repeated stresses with superimposed static stresses. Technical note 3495, NACA, USA, 1955.
- [10] Crossland, B., (ed.), *Effect of large hydrostatic pressures on the torsional fatigue strength of an alloy steel*, Int. Conf. on Fatigue of Metals, IMechE, 1986.
- [11] Findley, W.N., A theory for the effect of mean stress on fatigue of metals under combined torsion and axial load or bending - transactions of asme. *J Eng Industry*, **B81**, 1959.
- [12] Brown, M.W. & Miller, K.J., (eds.), *A Theory for Fatigue Failure Under Multiaxial Stress Strain Condition*, volume 187, IMechE, 1973.
- [13] Socie, D.F., Multiaxial fatigue damage models. *ASME*, **109**, pp. 293–298, 1987.
- [14] Fatemi, A. & Socie, D., A critical plane approach to multiaxial fatigue damage including outofphase loading, fatigue & fracture engng. *Mat Struct*, **11**, pp. 149–165, 1988.
- [15] McDiarmid, D.L., A general criterion for high cycle multiaxial fatigue failure. *Fatigue Fract Engng Mater Struct*, **14**, pp. 429–453, 1991.
- [16] Smith, K.N., Watson, P. & Topper, T.H., A stress-strain parameter for the fatigue of metals. *Journal of Materials*, **5**, pp. 767–778, 1970.
- [17] Kussmaul, K.F., McDiarmid, D.L. & Socie, D.F., *Fatigue under Biaxial and Multiaxial Loading*. Mech.

- Engineering Publications, 1991.
- [18] Karolczuk, A. & Macha, E., A review of critical plane orientations in multiaxial fatigue failure criteria of metallic materials. *Int J Fracture*, **134**, pp. 267–304, 2005.
  - [19] Papadopoulos, I.V., A new criterion of fatigue strength for out-of-phase bending and torsion of hard metals. *Int J Fatigue*, **16**, pp. 377–384, 1994.
  - [20] You, B.R. & Lee, S.B., A critical review on multiaxial fatigue assessments of metals. *Int J Fatigue*, **18**, pp. 235–244, 1996.
  - [21] Papadopoulos, I.V., Long life fatigue under multiaxial loading. *Int J Fatigue*, **23(10)**, pp. 839–849, 2001.
  - [22] Grübisic, V. & Simbürger, A., (eds.), *Fatigue under Combined Out-of-Phase Multiaxial Stresses*, Society of Environmental Engrs, Int. Conf. Fatigue Testing and Design, 1976.
  - [23] Dang Van, K., Griveau, B. & Message, O., On a new multiaxial fatigue limit criterion: Theory and application. *Biaxial and Multiaxial Fatigue, EGF 3*, eds. M.W. Brown & K.J. Miller, MEP, 1989.
  - [24] Papadopoulos, I.V., Critical plane approaches in high-cycle fatigue: On the definition of the amplitude and mean value of the shear stress acting on the critical plane. *Fatigue Fract Engng Mater Struct*, **21**, pp. 269–285, 1998.
  - [25] Papadopoulos, I.V., *A Review of Multiaxial Fatigue Limit Criteria*. ECJRC, 1992.
  - [26] Kakuno, H. & Kawada, Y., A new criterion of fatigue strength of a round bar subjected to combined static and repeated bending and torsion. *Fatigue Engng Mat Struct*, **2**, pp. 229–236, 1979.
  - [27] Bin, L., Santos, J.L.T. & Freitas, M., A unified numerical approach for multiaxial fatigue limit evaluation. *Mech Struct & Mach*, **28(1)**, pp. 85–103, 2000.
  - [28] Van, K.D., Sur la résistance à la fatigue des métaux. *Sciences et Technique de L'armement*, **47**, pp. 429–453, 1973.
  - [29] Deperrois, A., *Sur le Calcul de Limites D'Endurance des Aciers*. These de doctorat, Ecole Polytechnique, Paris, 1991.
  - [30] Duprat, D., Boudet, R. & Davy, A., (eds.), *A Simple Model to Predict Fatigue Strength with Out-of Phase Tension-Bending and Torsion Stress Condition*, 9<sup>th</sup> Int. Conf Fracture: Sidney - Australia, 1997.
  - [31] Mamiya, E.N. & Araujo, J.A., Fatigue limit under multiaxial loadings: On the definition of the equivalent shear stress. *Mechanics Research Communications*, **29**, pp. 141–151, 2002.
  - [32] Malcher, L. & Balthazar, J.C., (eds.), *An Analysis of the Ellipsoid Simplified Model for Determination of the Fatigue Strength in Biaxial/Triaxial Loading and Out-of-Phase*, 16<sup>o</sup> POSMEC - 16<sup>o</sup> Simpósio de Pós-Graduação em Engenharia Mecânica: Uberlandia - Brazil, 2006.
  - [33] Papadopoulos, I.V. & Van, K.D., Sur la nucleation des fissures en fatigue polycyclique sous chargement multiaxial. *Arch Mech*, **40**, pp. 759–774, 1988.
  - [34] Papadopoulos, I., Davoli, P., Gorla, C., Filippini, M. & Bernasconi, A., A comparative study of multiaxial high-cycle fatigue criteria for metals. *Int J Fatigue*, **19(3)**, pp. 219–235, 1997.